JOURNAL OF GEOPHYSICAL RESEARCH, VOL. 113, D21107, doi:10.1029/2007JD009461, 2008

Dynamical downscaling: Assessment of model system dependent retained and added variability for two different regional climate models

Burkhardt Rockel,[1] Christopher L. Castro,[2] Roger A. Pielke Sr.,[3] Hans von Storch,[1] and Giovanni Leoncini[4]

Received 5 October 2007; revised 3 August 2008; accepted 21 August 2008; published 5 November 2008.

[1] In this paper, we compare the retained and added variability obtained using the regional climate model CLM (Climate version of the Local Model of the German Weather Service) to an earlier study using the RAMS (Regional Atmospheric Modeling System) model. Both models yield similar results for their standard configurations with a commonly used nudging technique applied to the driving model fields. Significantly both models do not adequately retain the large-scale variability in total kinetic energy with results poorer on a larger grid domain. Additional experiments with interior nudging, however, permit the retention of large-scale values for both models. The spectral nudging technique permits more added variability at smaller scales than a four-dimensional internal grid nudging on large domains. We also confirmed that dynamic downscaling does not retain (or increase) simulation skill of the large-scale fields over and beyond that which exists in the larger-scale model or reanalysis. Our conclusions should be relevant to all applications of dynamic downscaling for regional climate simulations.

Citation: Rockel, B., C. L. Castro, R. A. Pielke Sr., H. von Storch, and G. Leoncini (2008), Dynamical downscaling: Assessment of model system dependent retained and added variability for two different regional climate models, *J. Geophys. Res.*, *113*, D21107, doi:10.1029/2007JD009461.

1. Introduction

[2] To obtain greater horizontally resolved information from long term global general circulation model (GCM) simulations, a downscaling of the results by statistical methods "statistical downscaling") or by high-resolution regional climate models (RCMs) ("dynamical downscaling") have been applied. Downscaling from global reanalysis data by RCMs as a cheap alternative to a high-resolution regional reanalysis has also been used [e.g., *Feser et al.*, 2001; *Miguez-Macho et al.*, 2004; *Kanamitsu and Kanamaru*, 2007; *Castro et al.*, 2007a, 2007b]. In both cases we want the downscaling technique to retain the large-scale features given by the global reanalysis and add information on the smaller scales.

[3] *Castro et al.* [2005] proposed four types of dynamic downscaling. Type 1, which is used for numerical weather prediction, remembers its real-world initial conditions, as do the lateral boundary conditions.

[4] In Type 2, the initial conditions in the interior of the model are "forgotten" but the lateral boundary conditions feed real-world data into the regional model (through the reanalyses in our study). In Type 3, a global model prediction, rather than a reanalysis, is used to create the lateral boundary conditions. The global model prediction, however, includes real-world data such as prescribed SSTs, sea ice coverage, etc. These internal climate system components are assigned and not predicted. This constrains the global model predictions such that some real-world data is still fed into the regional model through the lateral boundary conditions. In Type 4, a global model is run in which there are no prescribed internal climate system forcings. The coupling (interfacial fluxes) among the ocean-land-continental ice-atmosphere are all predicted.

[5] In this paper, we assess the value of dynamic downscaling using Type 2 simulations. *Castro et al.* [2005] investigated Type 2 dynamic downscaling in a suite of experiments for May 1993 using the RAMS model [*Pielke et al.*, 1992] to see how that model behaves in this respect. May 1993 was selected due to the strong baroclynic waves present during this time making this month particularly suitable to test any RCM. Both a commonly-used nudging to NCEP reanalysis data (i.e., nudging the grid boxes in a sponge zone at the boundaries [*Davies*, 1976]) and an interior nudging alternative were tested. They found that the interior nudging gives better results for large scales but at the expense of a reduced variability at smaller scales.

[6] Two questions arising from this study will be examined in this paper:

[1]Institute for Coastal Research, GKSS Research Centre, Geesthacht, Germany.
[2]Department of Atmospheric Sciences, University of Arizona, Tucson, Arizona, USA.
[3]CIRES/ATOC, University of Colorado, Boulder, Colorado, USA.
[4]Meteorology Department, University of Reading, Reading, UK.

0148-0227/08/2007JD009461$09.00

[7] 1. Can the results be confirmed using a different model system? and

[8] 2. What is the effect of a different interior nudging technique (i.e., the difference between a 4DDA internal nudging type and spectral nudging)?

[9] A recent study by *Xue et al.* [2007] investigated aspects of the ability to dynamically downscale and found that domain size, lateral boundary conditions, and grid spacing were crucial issues associated with dynamic downscaling. We will investigate this issue further in this paper under the aspect of internal spectral nudging. It has to be noted that with increasing domain size the RCM will exhibit to a greater extent the chaotic nature of the atmosphere. However, we did not investigate this in our present study in this paper.

[10] This study does not aim (as in the "Big Brother" experiment [*Denis et al.*, 2003]) to determine whether the downscaled simulation can recreate the variability that was removed by spatial filtering and generated the initial and boundary conditions for the little brother experiment.

[11] The main focus of our study is to investigate whether skill in variability is added on the small scales. Even though in the presented Type 2 simulations no skill in variability is added to the larger wavelengths, RCMs may predict large scale features better than global circulation models for Type 3 and Type 4 experiments. However, the latter has still to be investigated by similar experiment set ups. If their domain is made large enough to resolve the dynamics and physics which generate and propagate these large-scale systems.

[12] Type 2 downscaling, since the global analyses are based on real world data, provides the most accurate description of the large scale atmospheric features. Type 3 and 4 downscaling which are not constrained by such observations, will not be as skillful at replicating these features. This is because the Type 2 downscaling is strongly forced by lateral boundary conditions and interior nudging so as to conform closely to the observations on the spatial scales that are resolved by the global analyses.

[13] Type 3 downscaling has a much less influence from the large scale (any influence is just due to prescribing data for use in a global model simulation from surface boundary observations such as sea surface temperatures, vegetation and soil moisture, etc.), while Type 4 downscaling has no observational constraints. Type 2 downscaling therefore provides the maximum skill that is achievable in accurately simulating regional and smaller scale atmospheric features.

[14] We also investigate how different kinds of nudging (i.e., standard boundary relaxation, 4DDA type internal nudging, spectral nudging) affect the spectral distribution of variability in two model systems.

2. Model and Methods

[15] For our study we used the regional climate model CLM which is the climate version of the German Weather Service (DWD) numerical weather forecast model COSMO (consortium for small-scale modeling) formerly known as "Local Model" [*Steppeler et al.*, 2003]. For the simulations of May 1993 the model time step was 120 s for all experiments. We applied lateral boundary forcing according to the method of *Davies* [1976]. Data for initialization and the lateral boundaries used for the model simulations were taken from the forty year reanalysis (ERA40) [*Uppala et al.*, 2005] of the European Centre for Medium Weather Forecast (ECMWF) with a horizontal grid increment of about 125 km. For nudging in the interior domain (i.e., over the whole model domain) a spectral nudging technique [e.g., *Kida et al.*, 1991; *von Storch et al.*, 2000] can be applied.

[16] In the standard setup, the observed state is forced upon the model in a lateral boundary zone covering eight grid points using *Davies* [1976] classical "sponge" technique: The "interior" solution of the model, denoted Ψ, is brought closer to, or "nudged" to the observed state, denoted Ψ^*, by adding an adjustment or restoring term $\gamma \cdot (\Psi^* - \Psi)$, where the "nudging coefficient" γ takes largest values at the lateral boundary and decreases toward the interior of the integration domain. In the CLM γ decreases as a function of hyperbolic tangent and shows significant weight only for grid points with less than nine grid points distance from the boundaries. The nudging coefficient has units of 1/s. This standard approach is commonly used in regional weather forecasting and regional climate simulations. The "sponge" zone has been introduced to avoid reflection of traveling features at the boundaries. Inconsistencies stemming from internally generated features traveling toward the lateral boundaries and conflicting there with the prescribed conditions are dampened out in this manner.

[17] In the "spectral nudging" approach, the lateral "sponge forcing" is kept and an additional steering is introduced as described next.

[18] Consider the expansion of a suitable CLM variable:

$$\Psi(\lambda, \phi, t) = \sum_{j=-J_m, k=-K_m}^{J_m, K_m} \alpha_{j,k}^{m}(t) e^{ij\lambda/L_\lambda} e^{ik\phi/L_\phi} \tag{1}$$

with zonal coordinates λ, zonal wave numbers j and zonal extension of the area L_λ. Meridional coordinates are denoted by ϕ, meridional wave numbers by k, and the meridional extension by L_ϕ. t represents time. For CLM, the number of zonal and meridional wave numbers is J_m and K_m. A similar expansion is done for the analyses, which are given on a coarser grid. The coefficients of this expansion are labeled $\alpha_{j,k}^{a}$, and the number of Fourier coefficients is $J_a < J_m$ and $K_a < K_m$. The confidence we have in the realism of the different scales of the reanalysis depends on the wave numbers j and k and is denoted by $\eta_{j,k}$.

[19] The model is then allowed to deviate from the state given by the reanalysis conditional upon this confidence. This is achieved by adding "nudging terms" in the spectral domain in both directions

$$\sum_{j=-J_a, k=-K_a}^{J_a, K_a} \eta_{j,k} \left(\alpha_{j,k}^{a}(t) - \alpha_{j,k}^{m}(t) \right) e^{ij\lambda/L_\lambda} e^{ik\phi/L_\phi} \tag{2}$$

In the following, we will use the nudging terms dependent on height. That is, our confidence in the reanalysis increases with height. On the other hand, we leave the regional model more room for its own dynamics at the lower levels where we expect regional geographical features are becoming more important. The better the confidence, the larger the $\eta_{j,k}$-values and the more efficient the nudging term.

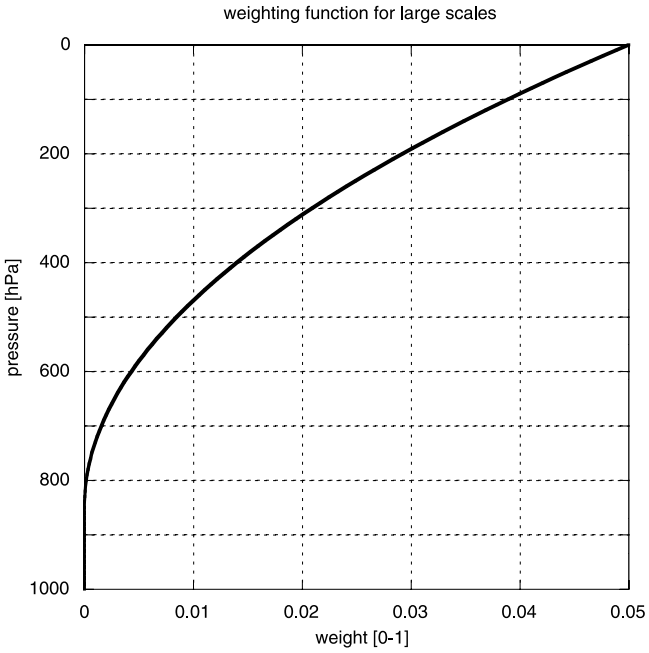

Figure 1. Weighting function η^0 of spectral nudging versus pressure height using a value for α of 0.05.

[20] In this study, we have applied nudging to the zonal and meridional wind components. Following *Giorgi et al.* [1993] we use a height-dependent nudging coefficient. Specifically, we use a pointwise nudging in case of excessively high wind speeds for preventing numerical instability

$$\eta^0(p) = \begin{cases} \alpha\left(1 - \dfrac{p}{850\,\mathrm{hPa}}\right)^2 & \text{for } p < 850\,\mathrm{hPa} \\ 0 & \text{for } p > 850\,\mathrm{hPa} \end{cases} \quad (3)$$

with p denoting pressure. Figure 1 shows the weighting function applied in this study.

[21] We have set $\eta_{j,k} = \eta^0$ for $j = 0, \ldots, nj$ in the north–south direction, $k = 0, \ldots, nk$ in the east–west direction and $\eta_{j,k} = 0$ otherwise. nj and nk are determined by

$$nk_m = \frac{nx_m * \Delta x_m}{4 * \Delta x_a} \quad (4)$$

$$nj_m = \frac{ny_m * \Delta y_m}{4 * \Delta y_a} \quad (5)$$

where nx_m and ny_m are the number of grid cells in the meridional and zonal direction, respectively. Δx_m, Δx_a and Δy_m, Δy_a are the grid mesh widths in the meridional and zonal direction, respectively. Subscript m and a denotes CLM and ERA40 reanalysis data, respectively.

[22] For the interior nudging test case we applied this nudging to the horizontal wind components u and v above 850 hPa with a height-dependent weighting function. As can be seen from Figure 1, the weighting is very light with a maximum of 0.05 at the top of the model. Grid data from the ERA40 reanalysis and the CLM are transferred into the spectral space where the values of u and v for the large wave numbers of the CLM are nudged by those of the reanalysis. All values for wavelengths larger than the one corresponding to the smallest physically resolved wavelength $4\Delta x$ [*Pielke*, 2002] of the reanalysis are nudged. The resulting fields are transferred back to the grid space. Table 1 summarizes the grid widths and the related maximum wave number $k^*_{\max}$ corresponding to $4\Delta x$. The spectral nudging is applied each model time step.

[23] To distinguish between the $k^*_{\max}$ of the reanalysis data and the CLM, we denote the first one with an upper case K and the second one with a lower case k (i.e., $K^*_{\max}$ and $k^*_{\max}$, respectively).

[24] Both models, RAMS and CLM, have the same boundary forcing method [*Davies*, 1976] implemented which is the most commonly used nudging in RCMs. However, RAMS and CLM differ substantially in how the additional nudging in the interior of the model domain is performed in our experiments. For RAMS, a four-dimensional assimilation is applied across the wavelengths resolved by the regional model which nudges the grid values of the prognostic variables toward those of the driving reanalysis. For the spectral representation this means that RAMS and the driving model are combined over the whole wavelength spectrum. The interior nudging applied in the CLM experiment is quite different since it does not perform nudging in the grid space but in the spectral space and nudges the large-scale wavelengths only. Therefore because of the height dependency and the small nudging coefficient, we leave the regional model more room for its own dynamics especially at the lower levels. *Weaver et al.* [2002] reached a similar conclusion using a configuration with weaker nudging and higher resolution, supporting the idea that by not nudging synoptic scale observations/reanalysis at the mesoscale, simulations can be improved.

[25] Model resolution in climate studies has improved recently due to increased computing power for both GCMs and RCMs. For example, in the project ENSEMBLES [*Hewitt and Griggs*, 2004] simulations for future scenarios with several RCMs will be performed on a 25-km horizontal grid mesh size which is half of the commonly applied resolution in prior experiments. To stay abreast of these changes, we applied an experimental setup which is one step higher in resolution than in the study by *Castro et al.* [2005]. However, we kept the same small and large domain size (see Figure 1 in the work of *Castro et al.* [2005]). A comparison of the setups for the basic experiments between *Castro et al.* [2005] and this study is compiled in Table 2.

[26] In a follow-on suite of experiments we repeated the basic experiments but applied spectral nudging to the same cases presented in Table 2.

[27] The first and main focus of our analysis is on the differences in the spectral distribution of variability in the two model systems. This is shown on the example of the column average total kinetic energy and column integrated moisture flux divergence MFC (see equations (13)–(14) in

Table 1. Maximum Wave Number for Different Grid Mesh Sizes

	Δx (km)	$k^*_{\max}$ (10^{-5} m^{-1})	$\log_{10}$ ($k^*_{\max}$)
ERA40	125	1.26	−4.90
CLM	100	1.57	−4.80
CLM	50	3.14	−4.50
CLM	25	6.28	−4.20

Table 2. Setup of Basic Experiments

Basic Experiment	Δx (km)	Domain	RCM Grid Dimensions	RCM Name
1	200	small	40 × 25	RAMS
2	100	small	80 × 50	RAMS, CLM
3	50	small	160 × 100	RAMS, CLM
4	25	small	320 × 200	CLM
5	200	large	80 × 50	RAMS
6	100	large	160 × 100	RAMS, CLM
7	50	large	320 × 200	RAMS, CLM
8	25	large	640 × 400	CLM

the work of *Castro et al.* [2005]). Since the kinetic energy is a function of v^2 the main contribution to the total column kinetic energy comes from values in the upper troposphere. The main contribution to the total column integrated moisture flux divergence comes from the planetary boundary layer values of MFC due to the high moisture values near the surface. Figure 2 illustrates the vertical distributions of kinetic energy and MFC.

[28] We compared the variability added by the CLM against ERA40 and not another model because ERA40 includes observations and is a better representation of reality than model output alone.

[29] The second focus is on the influence of adding internal nudging to the standard relaxation boundary nudging on the prediction of various quantities.

[30] We applied the same spectral analysis of the model variables as described by *Castro et al.* [2005] to determine the power spectrum $S(k)$ of the variables, where k is the wave number. The fractional change in spectral power $\Delta S(k)_{frac}$ is computed for each analysis time step (i.e., every 6 hours) as:

$$\Delta S(k)_{frac} = \begin{cases} \dfrac{S(k)_{m_1}}{S(k)_a} - 1, \text{ for basic experiments} \\ \dfrac{S(k)_{m_2}}{S(k)_{m_1}} - 1, \text{ for follow up experiments} \end{cases} \quad (6)$$

where a is the reanalysis, m_1 is the basic experiment without internal nudging, and m_2 is the follow-on experiment with internal nudging.

3. Results and Discussion

3.1. Variability

[31] Regarding differences in results of RAMS and CLM, we expect larger dissimilarities to occur in the MFC than in the kinetic energy. The MFC is mainly influenced by humidity near the Earth's surface and in the planetary boundary layer (PBL). Physical parameterizations and surface characteristics in the models play an important role on the moisture budget in this part of the atmosphere. Since RCMs typically differ in parameterization schemes implemented (as with RAMS and CLM), we can expect larger differences in MFC than in kinetic energy. Kinetic energy is mostly influenced by upper air wind speeds which are less sensitive (but not negligible) to parameterizations than the MFC.

[32] Figure 3 shows the fractional change in spectral power for the column-average total kinetic energy and the MFC as a mean over the last 15 days of May 1993. This figure compares to Figure 4 in the work of *Castro et al.* [2005]. For the kinetic energy the results from the basic model experiments look very similar. Both models show the same behavior in variability for wave numbers higher than K^*_{max}. K^*_{max} for the course grid model is denoted by a solid vertical line in all figures; the vertical dashed line shows the k^*_{max} of the 25-km CLM version. The higher the horizontal resolution the higher the added variability. For low wave numbers (less than K^*_{max}) the CLM retains about the same variability as the RAMS version with explicit microphysics and Kain-Fritsch scheme turned on.

[33] The MFC (Figure 3, right-hand side) in the CLM simulations shows the same features as the kinetic energy, but with an even larger variability for wave numbers larger than K^*_{max}. This is as expected since higher resolved surface characteristics lead to a greater variability in surface and near-surface atmospheric parameters. The results between CLM and RAMS are different for MFC. *Castro et al.* [2005] showed that the results from their experiments with the Kuo convection scheme are poorer than those with the Kain-Fritsch scheme. This partly explains the differences in the MFC shown in Figure 3 compared to Figure 4 of *Castro et al.* [2005]. For a more detailed study of the differences, an in-depth comparison of the different physical parameterizations in CLM and RAMS influencing the MFC would need to be performed. This is beyond the scope of the study completed here.

[34] The dotted curve in Figure 3 describes the fractional change in spectral power for the 25-km grid mesh on the large domain. Comparing the two curves for 25 km (large and small domains) we find that kinetic energy and MFC show a significantly different behavior. Kinetic energy is less retained at large scales on the large domain whereas

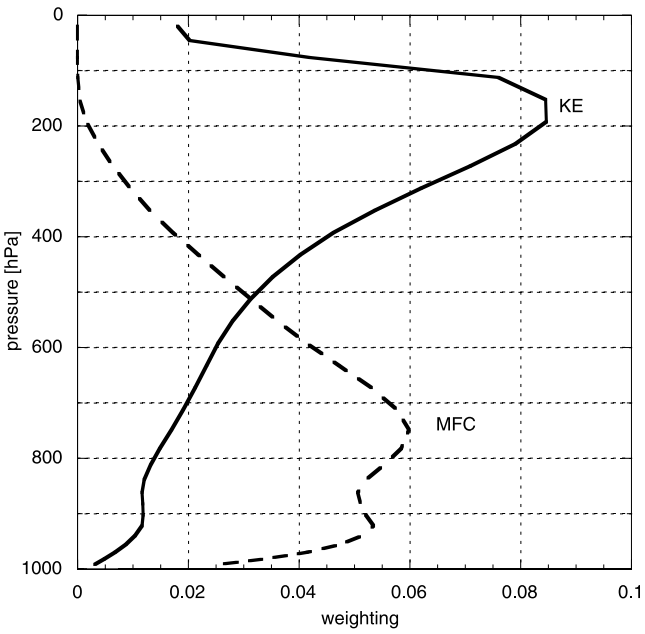

Figure 2. Vertical contribution of kinetic energy (KE) and moisture flux divergence (MFC) to the total vertically integrated values (this example is taken from the mean over the large-scale domain for the 50-km control simulation).

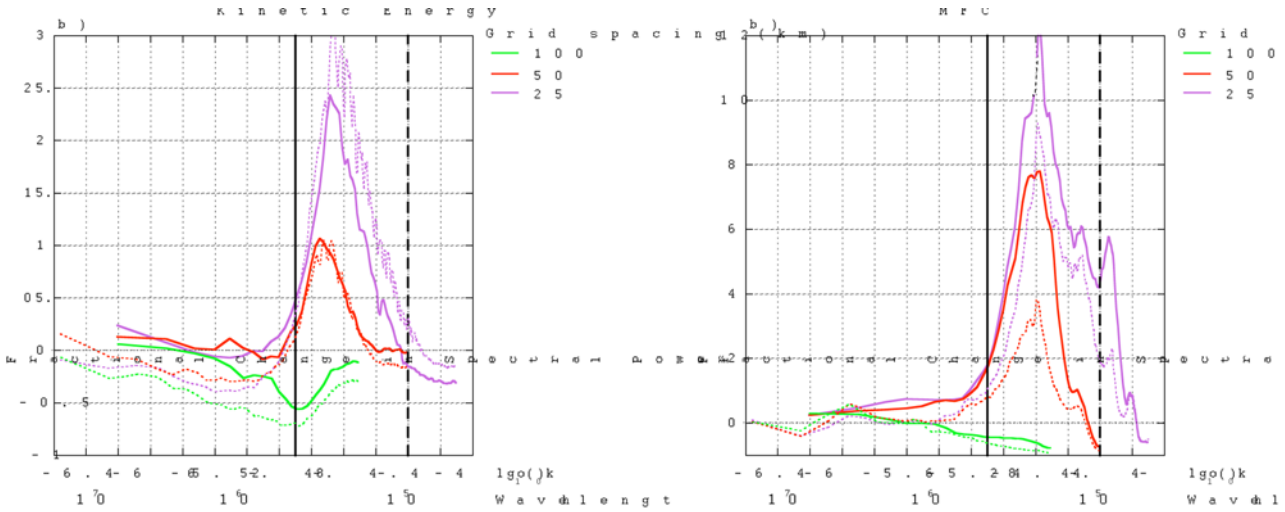

Figure 3. Fractional change in spectral power for column-average total kinetic energy (left) and integrated moisture flux convergence (MFC) (right). Results are for Δx = 100 km, 50 km, 25 km (green, red, and magenta lines, respectively) on the small domain. The dotted lines show the results for the large domain. k in units of m^{-1}. Wavelength in units of m. The vertical solid and dashed line show the K^*_{max} for the course grid model and the 25-km RCM version, respectively.

there is increased spatial variability on the smaller scales $k > K^*_{max}$. The MFC shows the opposite behavior. The value for the large-scale is better retained for the large area whereas we obtain a reduction in the added variability for wave numbers $k > K^*_{max}$. This holds also for the 50-km and 100-km experiments. For the kinetic energy the results for large wavelengths lead to the same conclusions for the 50-km and 100-km as for the 25-km version. The only difference appears for the short wavelengths where the variability on the large domain decreases stronger than the one on the small domain. This suggests a dependence of the variability on the area/number of grid points ratio.

[35] The different behavior of kinetic energy and MFC can be explained by the surface characteristics of the small and large domain. On the small domain, land areas are the main lower boundary, whereas by extending to the large domain, mainly ocean area is added. This means that the sea surface temperature (SST) plays an important role on the large domain. SST has a major influence on near-surface atmospheric humidity and therefore on MFC.

[36] Since the SST is prescribed by the large-scale reanalysis, it has a comparable effect as an interior grid scale nudging (i.e., in terms of spectral nudging it would be like nudging over all wavelengths not just the large ones). In terms of MFC, this means that the large-scale values are retained but added variability is suppressed for smaller scales.

[37] We also investigated the time evolution of the fraction of reanalysis kinetic energy (i.e., total kinetic energy from reanalysis data divided by total energy of the regional model) and the fraction of reanalysis kinetic energy variance for the whole May 1993 (no figures shown here). The variation of these fields is similar in both studies, except that the loss of energy in the RAMS simulations within the first 3 days of their simulation does not appear in the CLM simulation. RAMS does not recover from this loss but the values vary around this value during the rest of the simulation. The loss of energy in RAMS in the first 3 days of the simulation could be due to the cruder interior nudging of RAMS (with its inclusion of all regional model resolved wavelengths component) which damps the solutions right away.

[38] In addition to the basic experiments, we performed a follow-on experiment suite where the basic experiments were repeated but with additional interior nudging added. Figure 4 (solid curve) shows the results of the 25-km experiment on the small domain compared to the basic experiment applying equation (6) (this curve compares to Figure 9 shown in *Castro et al.* [2005]). Again, results in kinetic energy confirm the findings by *Castro et al.* [2005]. For large scales (i.e., wave numbers less K^*_{max}) the values for the RCM are pushed nearer to those of the global reanalysis which means that the value is better retained by applying interior nudging. Both RCMs show a reduction in added variability. The influence in the CLM results is less of a reduction in the added variability mainly due to the fact that in CLM only the large wave numbers are nudged.

[39] The influence on the MFC for the larger scales is similar in both models. As for the kinetic energy the interior nudging retains the value of the global reanalysis. However, there are major differences for the small scales between the CLM and RAMS results. RAMS reduces the added variability, whereas in CLM the added variability is nearly preserved. This is primarily due to the different kind of interior nudging.

[40] The interior nudging in the grid space as applied in RAMS is performed over the whole grid for the prognostic variables (wind, temperature, pressure, and water vapor), whereas in the CLM the interior nudging is applied in the spectral space for large wavelengths only and the nudging is applied only above the PBL and only to the wind components.

[41] The dashed curve in Figure 4 describes the results for the large domain. Here the behavior of the regional model at the large-scale is the same as for the small domain. The

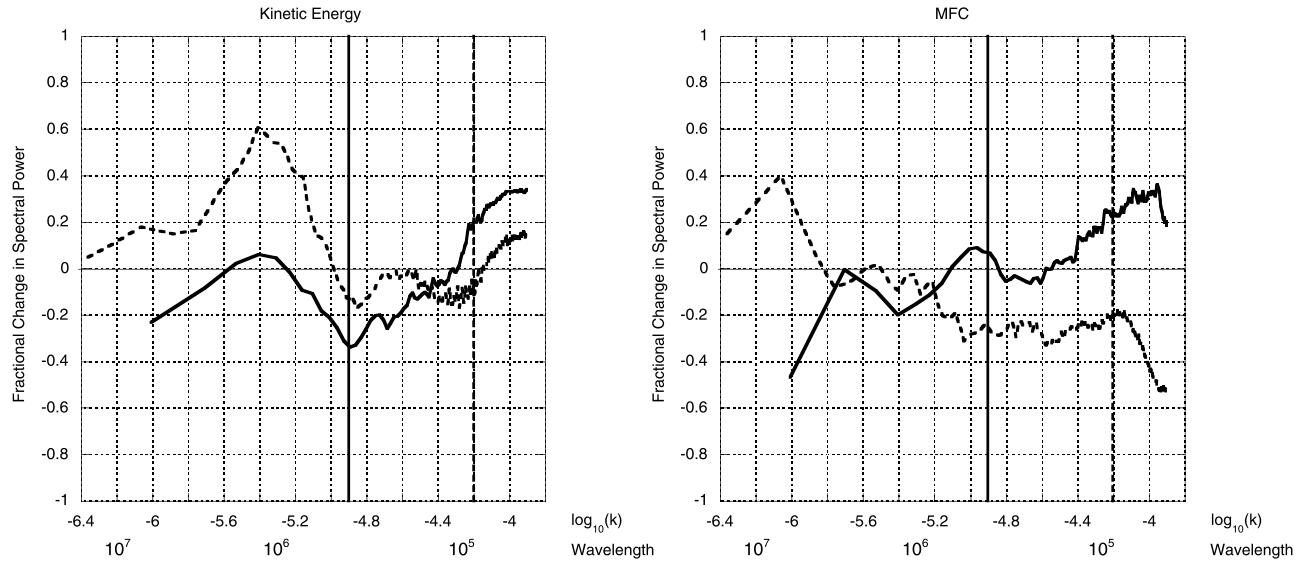

Figure 4. Fractional change in spectral power (spectral nudging vs. control) for column-average total kinetic energy (left) and integrated moisture flux convergence (MFC) (right) on the small domain (solid curve) and on the large domain (dashed curve) for $\Delta x = 25$ km. k in units of m^{-1}. Wavelength in units of m. The vertical solid and dashed line show the K^*_{max} for the course grid model and the 25-km RCM version, respectively.

interior nudging helps retain the large-scale values. However, there are differences on the smaller scales.

[42] For the kinetic energy the added variability is better retained for $k > K^*_{max}$ at values lower -4.5 for $\log_{10}(k)$ but poorer for larger wave numbers. The added variability for the MFC is no longer preserved, but decreases. The values of MFC depend on the gradients of the horizontal velocities and the absolute humidities, while the KE is calculated from the square of the velocities. A field that is derived from gradients (i.e., the MFC) will produce different scales of variability than a field which involves the original variables themselves (i.e., the KE). In the larger-scale domain, the gradient apparently becomes smeared more than the velocities themselves, and loses this variability. This can be either due to the greater region for internal damping as systems propagate in from the lateral boundaries, or that for this month, May 1993, the MFC is dominated by the large-scale signal, not by the mesoscale. For the latter only the better performance of the interior nudging allows this to show. The higher variability of the MFC at the smaller scales over the small domain compared to the large domain was a reaction to the excessive nudging due to the prescribed SST dominating the surface boundary condition of the large domain.

[43] Results for the 50-km grid mesh (not shown) are similar to those in the work of *Castro et al.* [2005, Figure 9]. The authors do not consider the 100-km grid mesh since the reanalysis data are on a grid of similar size (125 km). Therefore there are hardly any additional small scales to be compared.

3.2. Effect of Internal Nudging on Predicted Quantities

[44] Our investigation regarding the 500-hPa height difference without internal nudging (see Figure 5, top figures, compares to Figure 3 in *Castro et al.* [2005]) leads to the same results and conclusions as for the RAMS simulations. The greatest differences occur in regions of low pressure troughs off the west coast of North America, over the Hudson Bay and over the east Atlantic near the British Isles. Even the magnitudes of the differences are approximately the same. For the follow-on experiment with interior nudging, CLM results show less maximum differences ($\sim$10 m) compared to RAMS ($\sim$35 m) (see Figure 5, bottom figures, compared to Figure 8 in *Castro et al.* [2005]). This can be related to the fact that RAMS interior nudging is performed equally weighted across the wavelength spectrum resolved by the model, whereas the interior nudging of the CLM is performed as selective nudging with higher weights on the long-wave features. This keeps the CLM nearer to the reanalysis, at least above the PBL. Differences occur in the same regions for the small and large domain simulations and increase with domain size. Spectral nudging is able to nearly cancel out the differences independent of the domain size, i.e., differences for the simulations with spectral nudging are of the same order for the small and large domain.

[45] The interpretation of internal nudging on precipitation is not so straightforward as for the 500-hPa geopotential height. Precipitation is affected by other model specifics that have an impact at least on the same order as internal nudging. For example, *Castro et al.* [2005] showed the effect of different convection schemes in the RAMS model on precipitation prediction. Thus we expect the effect of internal nudging to be less dominant for precipitation than for the 500-hPa geopotential height.

[46] Figure 6 shows the precipitation amount for the second half of May 1993 over the United States calculated with the CLM with 25km grid mesh. The results may be compared to the precipitation for the same period from ERA40 reanalysis and from NCEP observations (see Figure 7).

[47] Despite higher precipitation amounts and higher spatial variability, three of the simulations show similar

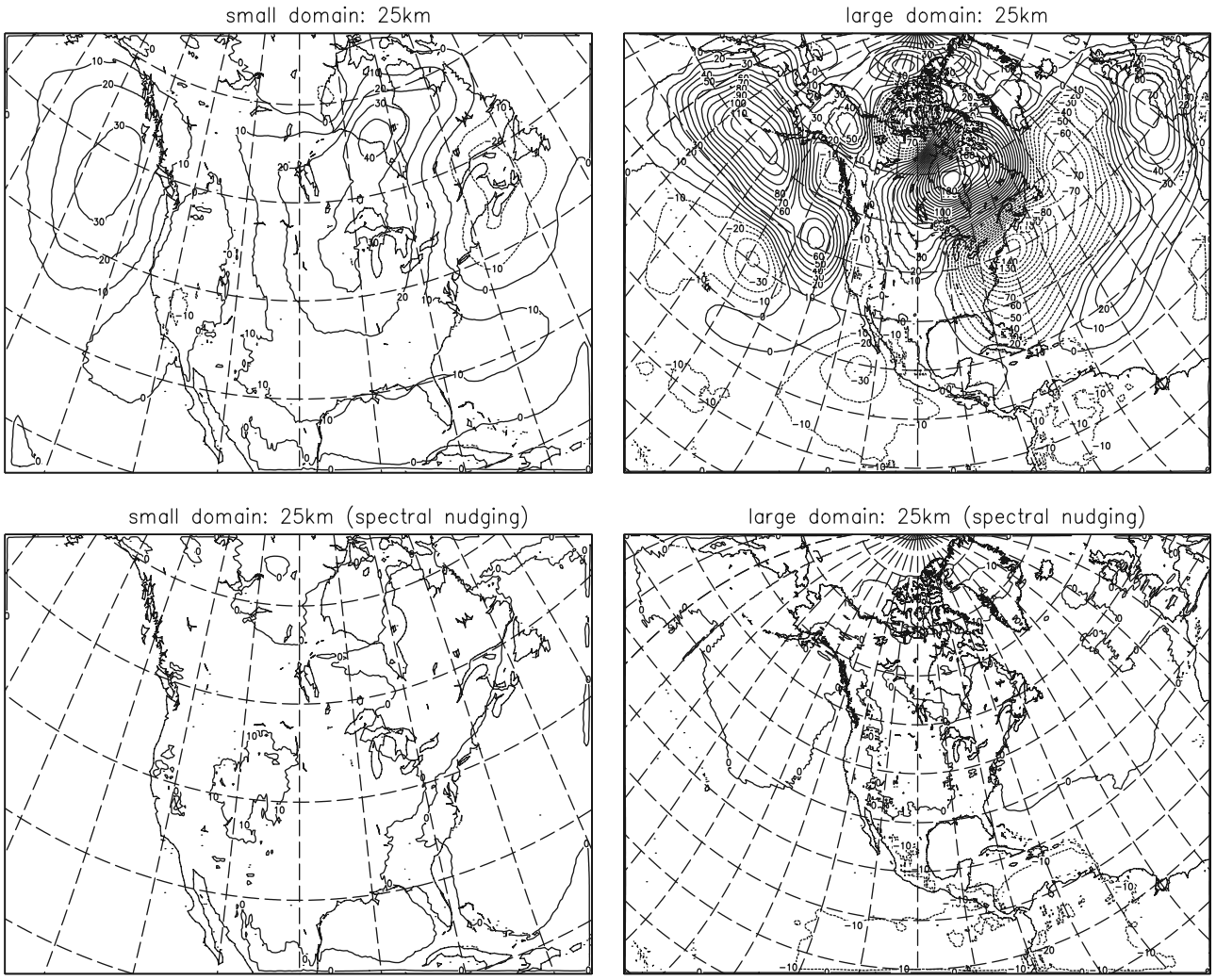

Figure 5. Difference in 500-hPa height as differences between the driving analysis and the CLM results for the second half of May 1993. Differences for simulations without and with spectral nudging are shown in the top and bottom rows, respectively. Isolines are drawn in 10-hPa intervals.

overall precipitation patterns as the driving ERA40 reanalysis (Figure 7). We can draw the same conclusion in comparing the internal nudging run with Kain-Fritsch convection scheme in the study by *Castro et al.* [2005] with the precipitation from the driving NCEP reanalysis.

[48] As expected the results are poorer for the simulation on the large domain without internal nudging (Figure 6, top right). There is no precipitation over South and Central U.S. Compared to the observations (Figure 7) the precipitation amount for the other simulations in the CLM is too high.

[49] In addition to these qualitative descriptions the correlation coefficients for the precipitation fields from 25 km CLM simulations in Figure 6 compared to NCEP observations give a quantitative measure for the performance of the different experiments. As expected the coefficient is lowest for the large area/no spectral nudging experiment. The correlation coefficient is 0 (i.e., no correlation at all) in that case. With spectral nudging turned on, the correlation is 0.43; slightly lower than for the small area with spectral nudging (0.46) but higher than for the small area with no spectral nudging version (0.37).

[50] We also compared the effect of internal nudging on two meter temperature and surface pressure. However, the effect of different planetary boundary layer parameterizations in the driving model and the regional model overrules the large-scale dynamics. Recently *Gustafson and Leung* [2007] came to the same conclusion in their study on regional downscaling. Nevertheless, the authors examined the results of two meter temperature and surface pressure but found no significant differences in the horizontal distribution between the versions with and without spectral nudging. Thus these quantities do not add sufficient additional information on the nudging issue studied for this paper.

[51] We did not perform any investigations on the spatial scales of these quantities. This should be considered in future studies on numerical downscaling. Techniques like the one by *Feser* [2006] can give additional information.

4. Conclusions

[52] The results for CLM presented here are similar to those found in the RAMS study by *Castro et al.* [2005] for

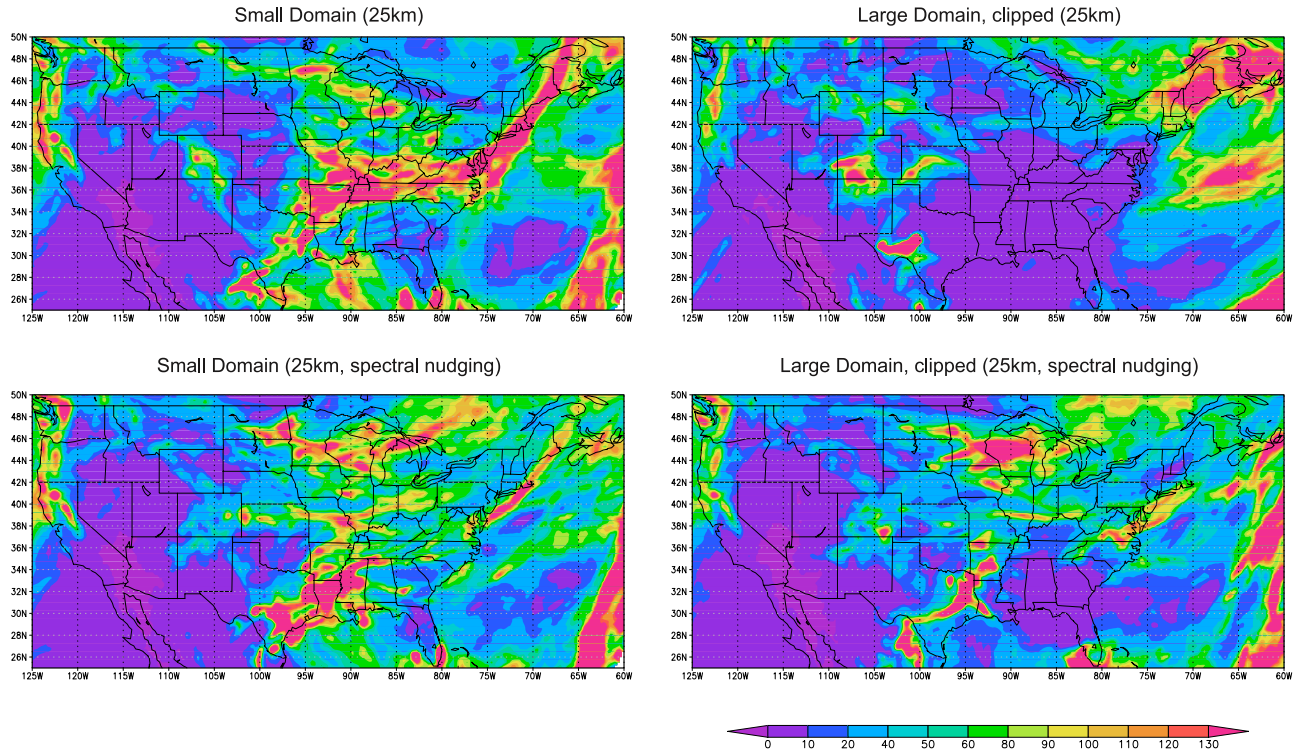

Figure 6. Precipitation results from CLM simulations for the second half of May 1993 without and with spectral nudging in the top and bottom rows, respectively.

the standard experiments, i.e., with commonly used nudging in a sponge zone after *Davies* [1976]. For the interior nudging experiments, the spectral nudging technique applied in the CLM simulations shows different results than the four-dimensional assimilation applied to the RAMS.

[53] Using spectral nudging as interior nudging gives less reduction in added variability of the smaller scales than grid nudging and is therefore the preferred approach in dynamic downscaling. The main reason is that spectral nudging is applied to large wavelengths and a subset of the dependent variables (i.e., the horizontal wind components) whereas grid nudging affects the entire resolved wave spectrum and each of the dependent variables. The results regarding the MFC suggest the effect to be largest for physical quantities in the lower troposphere. It has been shown that spectral nudging is preserving the variability of MFC at the small scales which is a major advantage over the full interior nudging as applied in the RAMS simulations.

[54] Spectral nudging in this study is applied every model time step (2 minutes). This emphasizes the fact that spectral nudging suppresses the variability at the small scales less than the broad spectrum grid nudging even more. For follow-on studies, the question arises whether there is an optimal time step for applying spectral nudging which still retains the large-scale values and results in even less suppression of the added variability.

[55] Our conclusions also demonstrates that the conclusions in the work of *Castro et al.* [2005] are not model

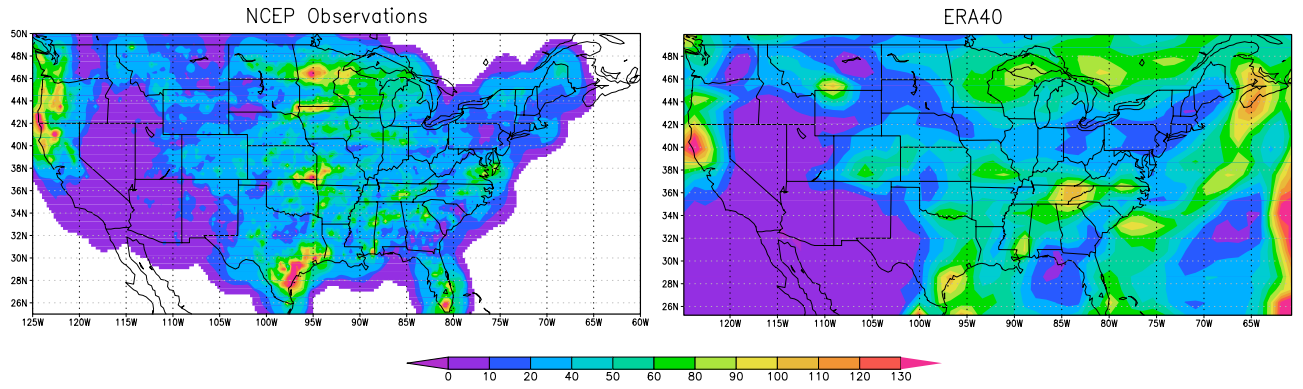

Figure 7. Precipitation from NCEP observation (left) and ERA40 reanalysis (right) for the second half of May 1993.

specific in that the utility of all regional climate models in downscaling global reanalysis primarily

> is not to add increased skill to the large-scale in the upper atmosphere, rather the value added is to resolve the smaller-scale features which have a greater dependence on the surface boundary.

[56] Furthermore,

> dynamical downscaling. . . does not retain value of the large-scale over and above that which exists in the larger global reanalysis. If the variability of synoptic features is underestimated or there is a consistent bias in the larger model, no increased skill would be gained by dynamical downscaling.

[57] Similar additional studies are needed to answer the question whether this holds (and if so under what conditions) for Type 3 (definition [see *Castro et al.*, 2005]) dynamic downscaling, as any real-world observational constraint on the simulation becomes less than with Type 2, and for Type 4 simulations, does not even exist at all.

[58] To prove this the experiments need to be done with dynamical downscaling of higher orders (i.e., GCM data). This is a question for future investigation–that is urgently needed. It is not included in the present article which is primarily to confirm the behavior described by *Castro et al.* [2005] with a different model system.

[59] **Acknowledgments.** We are grateful to ECMWF for using the ERA-40 as boundary conditions for our regional climate model. The part of this research performed by Chris Castro, Giovanni Leoncini, and Roger Pielke Sr. was funded in part by NOAA grant NA17RJ1228 amendment 6, NASA grant NGT5-30344, and U.S. Department of Defense Center for Geoscience/Atmospheric Research Grant at Colorado State University (under cooperative agreement W911NF-06-2-001 and DAAD19-02-2-0005 with the Army Research Laboratory). R.A. Pielke Sr. was also supported on this study through the University of Colorado in Boulder (CIRES/ATOC).

References

Castro, C. L. S., R. A. Pielke, and G. Leoncini (2005), Dynamical downscaling: Assessment of value retained and added using the Regional Atmospheric Modeling System (RAMS), *J. Geophys. Res.*, *110*, D05108, doi:10.1029/2004JD004721.

Castro, C. L. S., R. A. Pielke, and J. O. Adegoke (2007a), Investigation of the summer climate of the contiguous U.S. and Mexico using the Regional Atmospheric Modeling System (RAMS): part I: Model climatology (1950–2002), *J. Clim.*, *20*, 3844–3865.

Castro, C. L. S., R. A. Pielke, J. O. Adegoke, S. D. Schubert, and P. J. Pegion (2007b), Investigation of the summer climate of the contiguous U.S. and Mexico using the Regional Atmospheric Modeling System (RAMS): part II: Model climate variability, *J. Clim.*, *20*, 3866–3887.

Davies, H. C. (1976), A lateral boundary formulation for multi-level prediction models, *Quart. J. R. Meteorol. Soc.*, *102*, 405–418.

Denis, B., R. Laprise, J. Côté, and D. Caya (2003), Downscaling ability of one-way nested regional models: The big-brother experiment, *Clim. Dyn.*, *18*, 627–646.

Feser, F. (2006), Enhanced detectability of added value in limited area model results separated into different spatial scales, *Mon. Weather Rev.*, *134*(8), 2180–2190.

Feser, F., R. Weisse, and H. von Storch (2001), Multi-decadal atmospheric modeling for Europe yields multi-purpose data, *Eos Trans. AGU*, *82*(28), 305, doi:10.1029/01EO00176.

Giorgi, F., M. Marinucci, and G. Bates (1993), Development of second-generation regional climate model (RegCM2): part II. Convective processes and assimilation of lateral boundary condition, *Mon. Weather Rev.*, *121*, 2814–2832.

Gustafson, W., Jr., and L. R. Leung (2007), Regional downscaling for air quality assessment, *Bull. Am. Meteorol. Soc.*, *88*, 1215–1227.

Hewitt, C. D., and D. J. Griggs (2004), Ensemble-based predictions of climate changes and their impacts, *Eos Trans. AGU*, *85*(52), 566, doi:10.1029/2004EO520005.

Kanamitsu, M., and H. Kanamaru (2007), Fifty-seven-year California reanalysis downscaling at 10 km (CaRD10): part I. System detail and validation with observations, *J. Clim.*, *20*, 5553–5571.

Kida, H., T. Koide, H. Sasaki, and M. Chiba (1991), A new approach for coupling a limited area model to a GCM for regional climate simulations, *J. Meteorol. Soc. Jpn.*, *69*, 723–728.

Miguez-Macho, G., G. L. Stenchikov, and A. Robock (2004), Spectral nudging to eliminate the effects of domain position and geometry in regional climate model simulation, *J. Geophys. Res.*, *109*, D13104, doi:10.1029/2003JD004495.

Pielke, R. A., Sr. (2002), *Mesoscale Meteorological Modeling*, 2nd ed., 676 pp., Academic Press, San Diego, Calif.

Pielke, R. A., Sr., et al. (1992), A comprehensive meteorological modeling system - RAMS, *Meteorol. Atmos. Phys.*, *49*, 69–91.

Steppeler, J., G. Doms, H.-W. Bitzer, A. Gassmann, U. Damrath, and G. Gregoric (2003), Meso-gamma scale forecasts using the nonhydrostatic model lm, *Meteorol. Atmos. Phys.*, *82*, 75–96.

Uppala, S., et al. (2005), The ERA-40 re-analysis, *Quart. J. Roy. Meteorol. Soc.*, *131*, 2961–3012.

von Storch, H., H. Langenberg, and F. Feser (2000), A spectral nudging technique for dynamical downscaling purposes, *Mon. Weather Rev.*, *128*, 3664–3673.

Weaver, C., S. B. Roy, and R. Avissar (2002), Sensitivity of simulated mesoscale atmospheric circulations resulting from landscape heterogeneity to aspects of model configuration, *J. Geophys. Res.*, *107*(D20), 8041, doi:10.1029/2001JD000376.

Xue, Y., R. Vasic, Z. Janjic, F. Mesinger, and K. E. Mitchell (2007), Assessment of dynamical downscaling of the continental U.S. regional climate using the Eta/ SSi B regional climate model, *J. Clim.*, *20*, 4172–4193.

C. L. Castro, Department of Atmospheric Sciences, University of Arizona, Physics and Atmospheric Sciences Building, Room 520, 1118 East Fourth Street, Tucson, AZ 85721-0081, USA.

G. Leoncini, Meteorology Department, University of Reading, Earley Gate, P.O. Box 243, Reading RG6 6BB, UK.

R. A. Pielke Sr., CIRES/ATOC, University of Colorado, Stadium 255-16, Boulder, CO 80309, USA.

B. Rockel and H. von Storch, Institute for Coastal Research, GKSS Research Centre, Max-Planck-Strasse 1, 21502 Geesthacht, Germany. (burkhardt.rockel@gkss.de)